Analytica Chimica Acta 755 (2012) 100–107

Contents lists available at SciVerse ScienceDirect

Analytica Chimica Acta

journal homepage: www.elsevier.com/locate/aca

Modification of polypyrrole nanowires array with platinum nanoparticles and glucose oxidase for fabrication of a novel glucose biosensor

Guangqing Xu[a,b], Samuel B. Adeloju[a,*], Yucheng Wu[b], Xinyi Zhang[a]

[a] NanoScience and Sensor Technology Research Group, School of Applied Sciences and Engineering, Monash University, Churchill, Victoria 3842, Australia
[b] School of Materials Science and Engineering, Hefei University of Technology, Hefei 230009, China

HIGHLIGHTS

- Fabrication of well aligned PPyNWA of 20 nm diameter within AAO template.
- Improvement of electrochemical properties by decoration with PtNPs.
- Sensitive amperometric and potentiometric detection of glucose by adsorption of GOx on PPyNWA–PtNPs.
- Detection of as little as 5.6 μM glucose with potentiometric detection.
- Comparable or better detection limit and sensitivity than some glucose biosensors fabricated with nanomaterials.

GRAPHICAL ABSTRACT

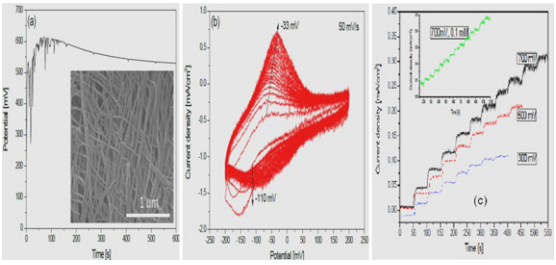

ARTICLE INFO

Article history:
Received 16 February 2012
Received in revised form
14 September 2012
Accepted 22 September 2012
Available online 1 October 2012

Keywords:
PPy nanowires
Pt nanoparticles
Biosensor
Electrochemical detection
Glucose

ABSTRACT

A novel glucose biosensor, based on the modification of well-aligned polypyrrole nanowires array (PPyNWA) with Pt nanoparticles (PtNPs) and subsequent surface adsorption of glucose oxidase (GOx), is described. The distinct differences in the electrochemical properties of PPyNWA–GOx, PPyNWA–PtNPs, and PPyNWA–PtNPs–GOx electrodes were revealed by cyclic voltammetry. In particular, the results obtained for PPyNWA–PtNPs–GOx biosensor showed evidence of direct electron transfer due mainly to modification with PtNPs. Optimum fabrication of the PPyNWA–PtNPs–GOx biosensor for both potentiometric and amperometric detection of glucose were achieved with 0.2 M pyrrole, applied current density of 0.1 mA cm^{-2}, polymerization time of 600 s, cyclic deposition of PtNPs from −200 mV to 200 mV, scan rate of 50 mV s^{-1}, and 20 cycles. A sensitivity of 40.5 mV/decade and a linear range of 10 μM to 1000 μM (R^2 = 0.9936) were achieved for potentiometric detection, while for amperometric detection a sensitivity of 34.7 μA cm^{-2} mM^{-1} at an applied potential of 700 mV and a linear range of 0.1–9 mM (R^2 = 0.9977) were achieved. In terms of achievable detection limit, potentiometric detection achieved 5.6 μM of glucose, while amperometric detection achieved 27.7 μM.

1. Introduction

The unique electronic, chemical, and physical properties of nanomaterials have continued to attract considerable interest for fabrication of chemical sensors and biosensors [1–5]. In particular, nanomaterials such as nanoparticles and carbon nanotubes have

* Corresponding author. Tel.: +61 399026450.
E-mail address: Sam.Adeloju@monash.edu (S.B. Adeloju).

0003-2670/$ – see front matter © 2012 Elsevier B.V. All rights reserved.
http://dx.doi.org/10.1016/j.aca.2012.09.037

been employed in several studies for electrode modification to improve the sensitivity and other performance of biosensors [6–8]. In recent years, one-dimensional nanoarrays, such as anodized titanium oxide (TiO_2) nanotubes array [9], and noble metal nanoarrays [10], including those obtained by using anodised aluminum oxide (AAO) templates, have also gained interest for fabrication of biosensors.

The ability to use these nanomaterials for fabrication of biosensors relies on the adequate immobilization of the desired biomolecules. The use of conducting polymers has proven to be one of the successful approaches for immobilization of enzymes on various nanomaterials because of their biocompatibility, ease of formation and high conductivity. In particular, polypyrrole (PPy) and polyaniline (PAn), both of which have been widely used for fabrication of numerous biosensors in the absence of nanomaterials, have attracted the most interest [11–14]. With the use of nanomaterials, the effective surface area can be increased significantly due to the formation of porous structures within the films. The formation of conductive polymer nanowires by this approach can enhance the performance of biosensors significantly. It has been reported that PPy and PAn nanowires can be obtained in a number of ways, including direct polymerization of pyrrole on glassy carbon electrode [15,16] and also growing on AAO template [17,18]. The deposition of conducting polymer nanowires on AAO templates is particularly significant for fabrication of biosensors because of their excellent biocompatibility, stability and high conductivity.

Many studies, particularly those based on fabrication of glucose biosensors, have focused their efforts on enhancement of the electrochemical detection of H_2O_2 through the modification of noble metal nanoparticles on TiO_2 nanotubes [19,20] and polypyrrole [21]. Other studies have indicated that it is possible to enhance the sensitivity of glucose biosensor with inclusion of carbon nanotubes (CNT) by deposition of Pt nanoparticles on CNT/TiO_2 nanotubes array by a factor of up to 5 times [2], on glassy carbon electrode by a factor of a least 2 [21], and on mesoporous carbon by a factor of 4–8 times [22]. However, this has never been attempted with PPyNWA or PAnNWA.

In this paper, the growth of well aligned PPy nanowires (PPyNWs) on AAO template is considered for improvement of the electron transfer of glucose biosensors. Furthermore, the possibility of using Pt nanoparticles (PtNPs) for decorating the PPyNWs is investigated for improvement of the performance of amperometric and potentiometric detection of glucose. The achievable performance for each mode of detection is compared to establish the best conditions for utilization of the PPyNWA–PtNPs–GOx biosensor for glucose detection. To this end, the effect of key parameters such as choice of pyrrole concentration, applied current density, potential sweep range, and scan rate was carefully evaluated.

2. Experimental

2.1. Chemicals

Glucose oxidase (type XS) extracted from *Aspergillus niger* was purchased from Sigma–Aldrich and used as received. The enzyme solution was prepared by dissolving GOx in 0.05 M phosphate buffer to give a 2000 U mL^{-1} solution and was kept at 4 °C in the fridge. Pyrrole, potassium chloroplatinate, sulphuric acid, potassium chloride, glucose, oxalic acid, phosphoric acid, chromic acid, and other chemicals, of analytical reagent grade, were purchased from Sigma–Aldrich Company. The pyrrole was distilled at about 130 °C prior to use, and was stored in a bottle covered with aluminium foil in the freezer to prevent UV degradation.

High purity aluminium foil (99.999%) was purchased from Beijing Cuibolin Non-Ferrous Technology Developing Co., Ltd, China. The supporting electrolyte was a 0.05 M phosphate buffer (pH 7) obtained by adjusting the ratio of Na_2HPO_4 and NaH_2PO_4.

2.2. Instruments

AAO templates were anodized with a direct-current power supply. Electrochemical polymerization and potentiometric detection were performed on a computerized potentiostat/galvanostat with a three-electrode cell, comprising of an Ag/AgCl (3 M KCl) reference electrode, a Pt/Ti wire auxiliary electrode, and an AAO template fixed on a gold disc working electrode. Cyclic voltammetric experiments were performed with VoltaLab PGZ 301 potentiostat–galvanostat (Copenhagen). Morphological study of the samples was performed with a JEOL JSM-6300F scanning electron microscope.

2.3. Fabrication of AAO template

AAO template was fabricated by a two-step anodization on an aluminum sheet. High purity aluminium discs (99.999%, 0.2 mm thick) of 22 mm diameter were used in the experiments, and 0.3 M oxalic acid was used as the electrolyte. The first anodization was performed by applying a potential of 45 V for 4 h at 0 °C, and the first oxide layer was removed by immersing samples in a mixed solution of phosphoric acid (0.5%) and chromic acid (0.5%) at 60 °C for 6 h. The second anodization was performed, after removing the first oxide layer, and then the aluminum on the reverse side was removed by immersing sample in 0.5 M copper chloride solution. The AAO template was immersed in 0.5 M phosphoric acid solution at 40 °C for 20 min to remove the barrier layer and enlarge the holes.

2.4. Formation of PPy nanowires array (PPyNWA) on AAO templates

The gold-disc electrode was polished with 5 μm aluminum oxide on a soft polishing pad to remove any film and washed thoroughly with Milli-Q water. The electrode was dried with fibre-free tissue paper. The AAO template was made conducting by vacuum-deposition of a gold layer on it. The template was then cut into a small size and fixed on the surface of the gold working electrode. The PPyNWA were formed by galvanostatic polymerization of pyrrole in a monomer solution which contained varying pyrrole concentration and 0.1 M KCl at different applied current density from 0.05 mA cm^{-2} to 0.3 mA cm^{-2} for 600 s.

After the formation of PPy, the electrode was washed several times with Milli-Q water to remove residual monomer solution. Then the electrode was placed in a 0.5 M NaOH solution to partly remove AAO template and was subsequently washed thoroughly with Milli-Q water.

2.5. Deposition of PtNPs on PPyNWA and adsorption of GOx

PtNPs were electrochemically deposited on the PPyNWA by cyclic voltammetric scanning from −200 mV to 200 mV in an electrolyte which contained 0.5 M H_2SO_4 and 5 mM K_2PtCl_6 at different scan rates and number of cycles.

The resulting PtNPs modified PPyNWA (PPyNWA–PtNP) was rinsed with Milli-Q water. The adsorption of enzyme was achieved by immersing the PPyNWA–PtNP electrode in 2000 U mL^{-1} GOx solution overnight at 4 °C. The electrode was then washed with Milli-Q water to remove residual free enzyme and was stored in a buffer solution at 4 °C.

2.6. Detection of glucose

The potentiometric detection of glucose was performed in a two-electrode cell with the PPyNWA–PtNP–GOx biosensor as the working (indicator) electrode and an Ag/AgCl (3 M KCl) reference electrode in 2 mL phosphate buffer solution (0.05 M, pH 7). Once a steady-state potential was reached, 20 μL glucose standard solution was added and the addition was repeated as many times as required.

The amperometric detection of glucose was performed in a three-electrode cell with the PPyNWA–PtNP–GOx biosensor as the working electrode in 2 mL buffer solution. The applied potential was determined from the cyclic voltammograms.

3. Results and discussion

3.1. Galvanostatic polymerization of pyrrole and modification with PtNPs

The gold-plated AAO template prepared in Section 2.4 was immersed in a pyrrole solution (between 0.1 M and 0.5 M) for 30 min to allow the solution to fill the holes of the template prior to growing the PPyNWA. On commencement of the polymerization the electrode potential fluctuates dramatically, decreasing to as low as 300 mV due to the irregular surface of the gold layer, as well as the difficulty of the monomer to diffuse into the nano-holes. Fig. 1a shows the chronopotentiogram obtained for the growth of PPyNWA on an AAO template with an applied current density of 0.2 mA cm^{-2}. Evidently, the fluctuation of the electrode potential diminished (after 150 s) with time and the potential became more stable at around 530 mV. The inset in Fig. 1a shows that PPy nanowires (PPyNWs) are grown uniformly from the holes of the AAO template with a diameter of about 20 nm. This diameter is much smaller than those of the holes (around 100 nm in diameter) and, thus, indicates that PPyNWs grew freely in the template instead of growing along the wall of the hole.

Fig. 1b shows the repeated cyclic voltammograms (CVs) obtained during subsequent deposition of PtNPs on PPyNWA between −200 mV and 200 mV at a scan rate of 50 mV s^{-1}. The observed current noise in the CVs for the PtNP deposition was due to two reasons: (a) attachment of the deposited PtNPs to the PPy nanowires array – it is well known that finely divided Pt is usually deposited by this electrochemical approach [23]. Weak or poor contact between the PtNPs and the PPy, as well as any nanowires not fully coated with PPy may contribute to the observed current noise. One way of improving on this is to entrap GOx with PPy on top of the PtNPs; and (b) while the current density ranged from −2 mA cm^{-2} to 1 mA cm^{-2}, the surface area of the electrode was only 0.0208 cm^2. As the current was between −40 μA and 20 μA, small variations will be more noticeable. Nevertheless, it was obvious that a reduction–oxidation couple was observed at about −110 mV and −50 mV for the deposition of PtNPs on the PPyNWA. The reduction peak remained stable at −110 mV, and peak current increased with time. However, the oxidation peak potential shifted from −50 mV to −33 mV with increasing number of cycle as a consequence of the increasing PtNPs thickness, and the peak current increased with repeated cycles. The increasing reduction and oxidation peak currents confirmed the formation of PtNPs on PPyNWA. Previous studies [23–25] have also indicated that the observed reduction peak at −110 mV is associated with formation of metallic platinum. For example, Lingane [23] reported on the chronopotentiometric reduction of $PtCl_6^{2-}$ at about −100 mV vs SCE. He observed anodic and cathodic chronopotentiometric waves of approximately equal transition times. He suggested that these correspond, respectively, to the oxidation of Pt(II) to the Pt(IV) and reduction to Pt(0). He also noticed that finely divided platinum were deposited on the electrode surface.

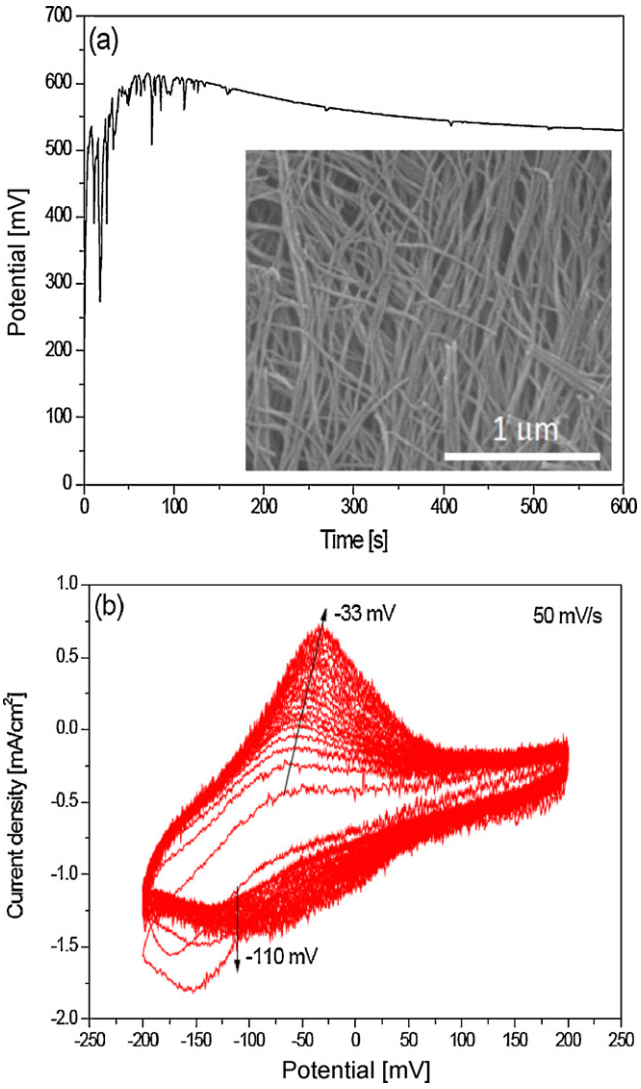

Fig. 1. Fabrication of PPyNWA–PtNPs. (a) Chronopotentiogram obtained for growth of PPyNWA, the insert is the SEM view of PPyNWA (23,000×). [Py] = 0.2 M, [KCl] = 0.1 M, current density is 0.2 mA cm^{-2} and time is 600 s; (b) CV deposition of PtNPs on PPyNWA. Potential range from −200 mV to 200 mV, scan speed is 50 mV s^{-1} and number of cycles is 20.

3.2. Electrochemical characterization of PPyNWA electrodes in presence of PtNPs and GOx

To further study the electrochemical properties of the PPyNWA–PtNPs electrode, two additional electrodes which contained GOx were prepared in the absence and presence of PtNPs for glucose detection. Fig. 2 shows the cyclic voltammograms obtained at PPyNWA–GOx, PPyNWA–PtNPs–GOx and PPyNWA–PtNPs electrodes in a phosphate buffer solution in the absence and presence of glucose at a scan rate of 10 mV s^{-1}. Curves (a) and (b) in Fig. 2(i) show the difference in the electrochemical behaviour of PPy–GOx film in phosphate buffer in absence and presence of glucose. Almost no change can be observed in the CVs with the addition of 10 mM glucose, except for a little decrease in the cathodic current at −610 mV, which indicates that PPy–GOx did not give a notable response to glucose. In contrast, curves (c) and (d) in Fig. 2(ii) compare the CVs of PPy–Pt–GOx in absence and presence of glucose. When 10 mM glucose was added to the buffer solution, the

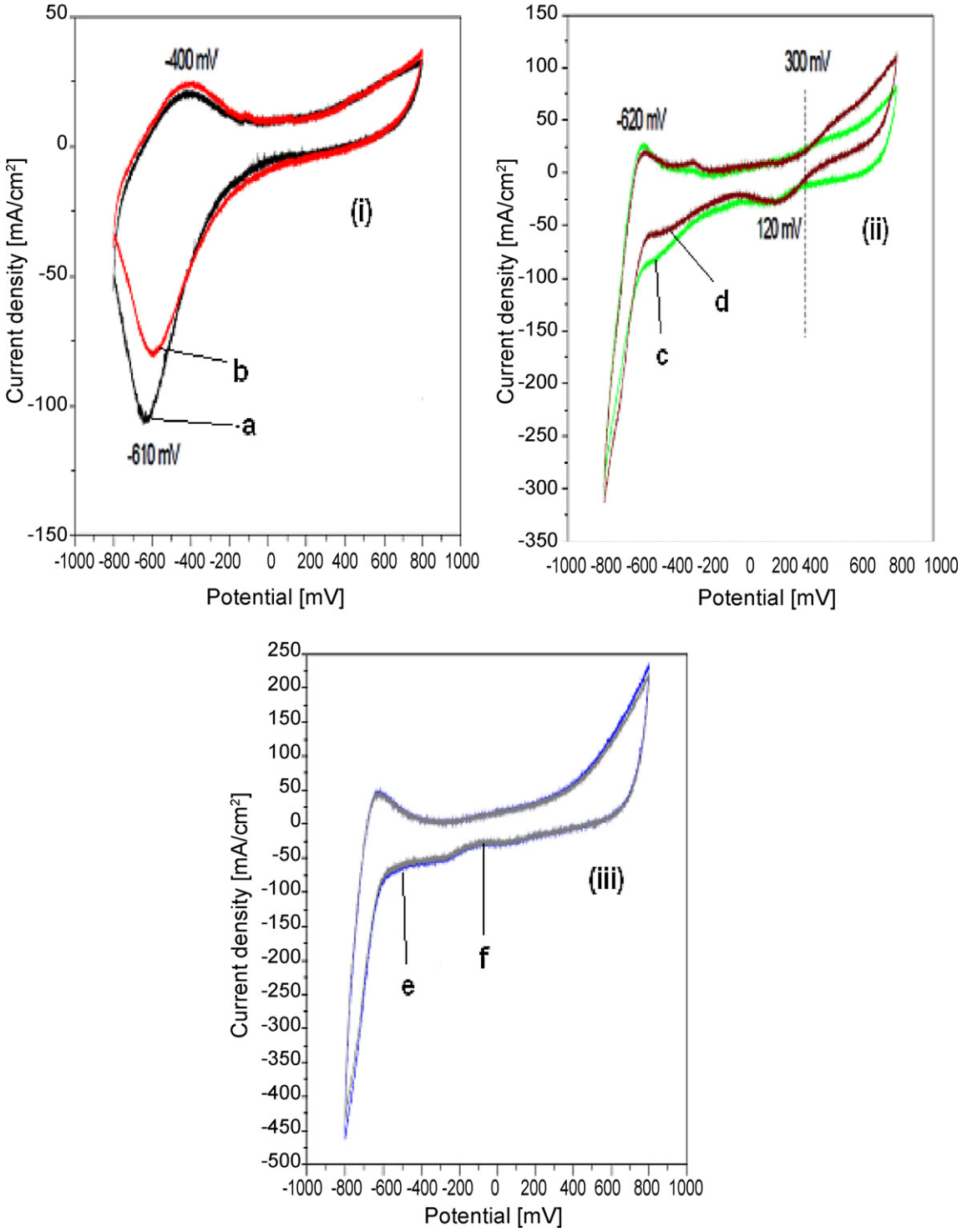

Fig. 2. Cyclic voltammograms of (i) PPyNWA–GOx, (ii) PPyNWA–PtNPs–GOx, and (iii) PPyNWA–PtNPs in buffer and in presence of 10 mM glucose. Scan rate: 10 mV s^{-1}; 0.05 M phosphate buffer (pH 7.0).

anodic current obtained with the PPy–Pt–GOx electrode increased at potentials higher than 300 mV, accompanied by a little decrease in the cathodic current. Curves (e) and (f) in Fig. 2(iii) show the CVs of PPy–Pt in 0.05 M buffer solution in absence and presence of 10 mM glucose. There was no observable difference in the two curves and, thus, indicates that PPyNWA–PtNPs did not give response to glucose in absence of GOx.

The effect of modification of the PPyNWA with PtNPs on its electrochemical behaviour is obvious from comparison of Fig. 2(i) with Fig. 2(ii). In the absence of PtNPs (Fig. 2(ii)), a reduction peak at −610 mV and an oxidation peak at −400 mV were obtained with a PPyNWA–GOx electrode placed in phosphate buffer. These peaks are consistent with those reported by Adeloju and Moline [26]. No other peaks were present, and thus indicate that there is no direct electron transfer between GOx and PPyNWs. However, at a PPy–NWA–PtNPs–GOx electrode (Fig. 2(ii)), both the anodic and cathodic currents increased substantially. The reduction current at potentials lower than −600 mV and the oxidation peak at −620 mV

were due to the electrochemical adsorption and desorption of hydrogen on Pt surface.

Fig. 2(iii) shows the CVs obtained with PPyNWA–PtNPs electrode which did not contain GOx. A comparison of the CVs with those obtained with PPy–NWA–PtNPs–GOx electrode (Fig. 2(ii)) reveals that there is only a common cathodic shoulder peak which appeared between −300 mV and −500 mV on both sets of CVs. Furthermore, it was noted that the presence or absence of glucose had no effect on the CVs (Fig. 2(iv)) obtained with the PPyNWA–PtNPs electrode. In contrast, the presence of GOx in the electrode (as PPyNWA–PtNPs–GOx electrode) did not only reduce the magnitude of the anodic and cathodic current by 53% and 32%, respectively, but also reveal notable differences in the absence and presence of glucose. As shown in Fig. 2(iii), when 10 mM glucose was added to the buffer solution, the anodic current increased by 27 mA cm^{-2} at potentials higher than 300 mV, accompanied by a decrease of 23 mA cm^{-2} in the cathodic current. This observation clearly indicates that the catalytic oxidation of glucose occurs readily in the presence of the immobilized GOx. The mechanism of the catalytic oxidation of glucose by the immobilized GOx can be explained by the following electrode reactions [22]:

$$\text{Glucose} + O_2 \xrightarrow{\text{GOx}} \text{Gluconic acid} + H_2O_2$$

$$H_2O_2 + 2H^+ + 2e^- \xrightarrow{\text{electrode}} 2H_2O\,(\text{cathodic current response})$$

$$2H_2O_2 \xrightarrow{\text{electrode}} H_2O + 2H^+ + 2e^-\,(\text{anodiccurrent response})$$

In addition to the observed anodic and cathodic current changes, three distinct additional peaks; 2 anodic at 500 mV and −340 mV, and 1 cathodic at 120 mV; were evident when CVs were obtained with the PPyNWA–PtNPs–GOx electrode in presence of glucose (Fig. 2(iii)). The anodic peak at about 500 mV and the cathodic peak at 120 mV were clearly associated with the catalytic oxidation of glucose and possibly due to the oxidation and reduction of peroxide generated by the enzymatic reaction. The presence of PtNPs has been previously shown to improve electrocatalytic activity [27].

As illustrated in Fig. 2(ii), the immobilized enzyme on PPyNWA–GOx electrode has the same catalytic effect on glucose as the enzyme immobilized on the PPyNWA–PtNPs–GOx electrode. This is evident from the suppression of the cathodic peak at −610 mV (Fig. 2(ii)), but lacked sensitivity to the H_2O_2 produced from the catalytic reaction. This view is well supported by the absence of the anodic peak or current increase at 500 mV and a cathodic peak at 120 mV observed in Fig. 2(iii). Overall, it can be concluded that the electrochemical reactivity and conductivity of PPyNWs modified with PtNPs were much better than those in which the nanoparticles were absent, as reflected by the number of peaks and the current magnitude. This is again consistent with the reported improvement of electrocatalytic activity when PtNPs are present [27]. Furthermore, as shown in Fig. 2(iii), the CVs obtained with the PPyNWA–PtNPs–GOx electrode in presence of glucose clearly indicates that a larger current response was obtained at potentials more positive than 300 mV. Furthermore, the hydrogen peroxide generated during the enzymatic reaction at the PPyNWA–PtNPs–GOx electrode gave potentiometric response which decreased with increasing glucose concentration. To fully appreciate the analytical utility of the PPyNWA–PtNPs–GOx biosensor, it was necessary to further optimized the biosensor for both amperometric and potentiometric detection of glucose.

3.3. Optimization of the PPyNWA–PtNPs–GOx biosensor

Fig. 3a shows the effect of the different current density employed for the growth of PPyNWA on the potentiometric and amperometric responses obtained for glucose. Evidently, the use of a current density of 0.1 mA cm^{-2} to grow the PPyNWA gave optimum amperometric and potentiometric response for glucose. At a lower current density (less than 0.1 mA cm^{-2}), the resulting PPyNWs were too short and difficult to expose from the AAO hole when the template was partly removed. This limited the adsorption of GOx and consequently affected glucose detection. The lower potentiometric response observed when current density above 0.1 mA cm^{-2} was used for the growth of the PPyNWs was due to an increase in nanowire length and thickness which increases the diffusion and electron transfer barriers of hydrogen peroxide.

The growth of PPyNWs with different pyrrole concentration had less effect on the glucose response obtained with the PPyNWA–PtNPs–GOx biosensors. In particular, the glucose responses obtained by potentiometric detection were not much different and the optimum response was obtained when the PPyNWs were grown with 0.2 M Py for both amperometric and potentiometric detection (Fig. 3b). At lower pyrrole concentration, the diffusion of pyrrole monomer was low and, hence, produced inadequate coverage of the electrode and gave low response to glucose. Beyond 0.2 M Py, the increased PPy film thickness and associated increase in diffusion barrier contributed to the observed reduction in the magnitude of the glucose response. Although the variation in the amperometric response obtained with PPyNWs formed with 0.2 M Py was slightly higher than for those formed in the presence of higher Py concentration, the considerable difference in the amperometric response (>100%) compensates for the slight variation. Interestingly, for potentiometric detection, there was no significant variation in the response obtained with PPyNWs prepared with ≥0.2 M Py.

Fig. 3c shows the influence of potential scan rate used for the deposition of PtNPs on the response of the PPyNWA–PtNPs–GOx biosensor to glucose. Evidently, both the amperometric and potentiometric response increased with the increasing scan rate from 25 mV s^{-1} to 50 mV s^{-1}. However, beyond a scan rate of 50 mV s^{-1} the glucose response obtained by both detection modes decreased considerably due to the increased thickness and particle size of the PtNPs. Consequently, an optimum scan rate of 50 mV s^{-1} was used for the deposition of the PtNPs on the PPyNWA.

Furthermore, both the amperometric and potentiometric response of glucose obtained with the PPyNWA–PtNPs–GOx biosensor increased, as shown in Fig. 3d, with the number of CV cycles used for the deposition of PtNPs over the PPyNWA up to 20 cycles. Beyond 20 cycles, the rapid decline in the response was due to increased PtNPs thickness and particle size. This may lead to formation of a Pt film over the PPyNWA and may block the adsorption of enzyme, as well as increase the diffusion barrier to the catalytic product and, thus, reduce the sensitivity of the response. Consequently, 20 cycles of CV was used as optimum for deposition of PtNPs over PPyNWA.

In summary, the optimum conditions established for fabrication of the PPyNWA–PtNPs–GOx biosensor for sensitive amperometric and potentiometric detection of glucose were: PPy film formation with 0.2 M Py, applied current density of 0.1 mA cm^{-2}, and polymerization time of 600 s; PtNPs deposition within −200–200 mV at a scan rate of 50 mV s^{-1}, and 20 CV cycles; enzyme adsorption with 2000 U mL^{-1} GOx for 15 h.

3.4. Analytical performance

Fig. 4a shows the typical chronopotentiograms obtained for increasing glucose concentrations with the optimized PPyNWA–PtNPs–GOx biosensor. The potentiometric response decreased sharply with each addition of glucose and took a long time (more than 100 s) to achieve stabilization, especially at lower glucose concentration. A plot of potential change versus

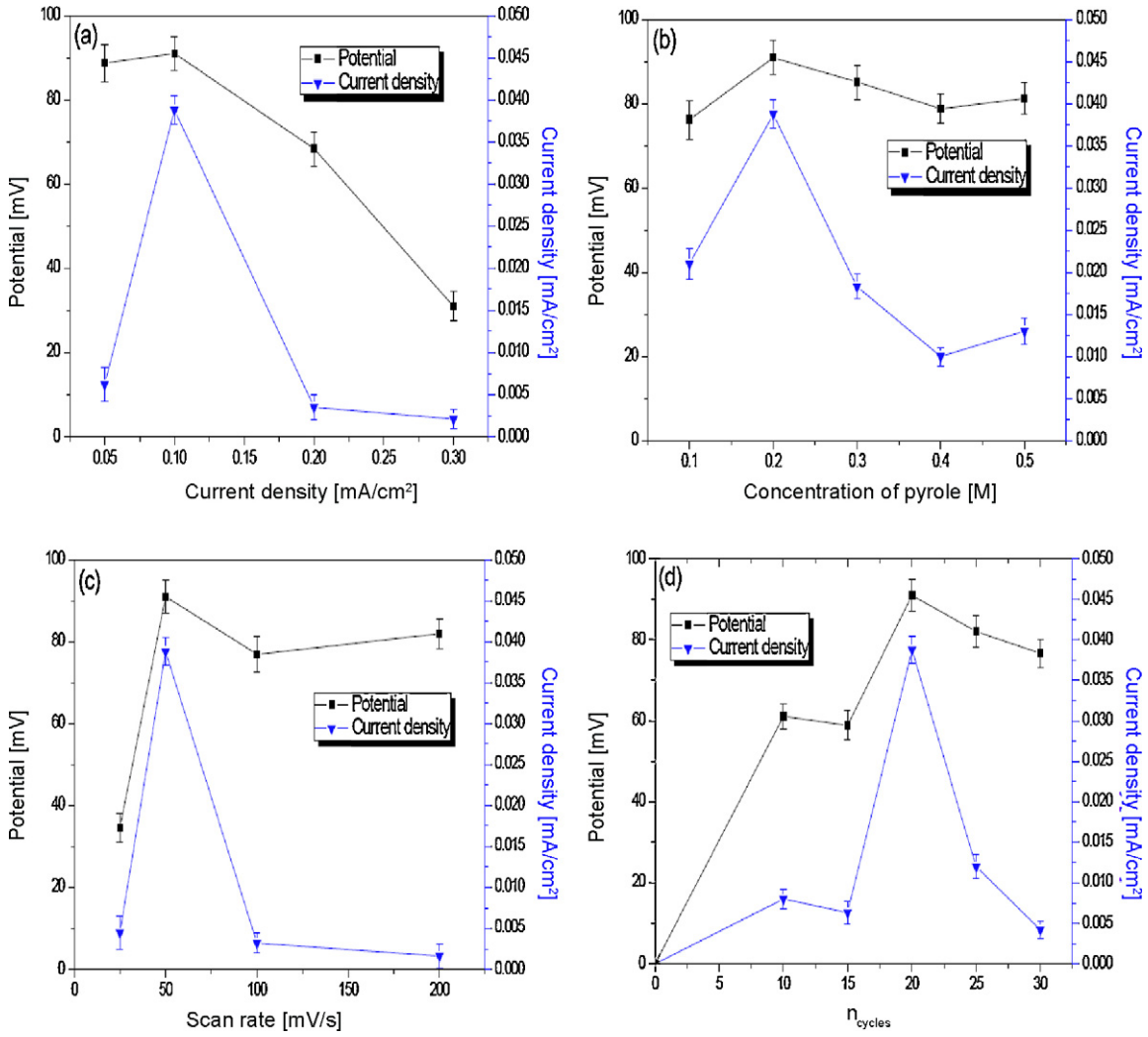

Fig. 3. Effect of (a) current density of polymerization, (b) concentration of pyrrole, (c) scan rate of CV deposition and (d) number of cycles on the potentiometric and amperometric detection of glucose with PPyNWA–PtNPs–GOx biosensor. Applied potential is 700 mV for amperometric detection; current density for polymerization is 0.1 mA cm^{-2}; [Py] = 0.2 M; scan rate for PtNPs deposition is 50 mV s^{-1} and 20 CV cycles.

$-\log[_{glucose}]$ (Fig. 4b) gave a Nernstian behaviour with a slope of 40.5 mV/decade and a linear concentration range from 10 μM to 1 mM (R^2 = 0.9936). The minimum detectable concentration of glucose achieved with the PPyNWA–PtNPs–GOx biosensor was 10 μM and the calculated detection limit (3σ) was 5.6 μM. Although the sensitivity achieved with this biosensor is not as good as that achieved (~90 mV/decade) with an ultra-thin PPy–GOx film biosensor [26], the detection limit is superior to those achieved with other glucose biosensors which employed nanomaterials such AuNW (46 μM) [28], Au modified CNT (20 μM) [29], and PPyNT (108 μM) [30].

Fig. 4c shows typical amperometric responses obtained at different applied potentials with the PPyNWA–PtNPs–GOx biosensor to successive additions of glucose in a phosphate buffer solution. The upper left inset shows the increase in amperometric response to successive increase in the lower glucose concentration range. The anodic current increases stepwise with successive injection of glucose, and the rapid response time (ca. 7 s) to changes in glucose concentrations indicate excellent electrocatalytic behaviour of the PPyNWA–PtNPs–GOx biosensor. It was obvious that the use of higher applied potential (700 mV) gave optimum glucose response. Fig. 4d shows that the amperometric response obtained with the PPyNWA–PtNPs–GOx biosensor at this applied potential increases linearly with glucose concentration from 0.1 mM to 9 mM (R^2 = 0.9977). From the calibration plot, a linear relationship was obtained within this concentration range as illustrated in Fig. 4d. The sensitivity of the PPyNWA–PtNPs–GOx biosensor obtained with an applied potential of 700 mV was 34.7 μA cm^{-2} mM^{-1}, which is much higher than those of other glucose biosensors which employed nanomaterials such as Pt modified PPy–GOx at 9.9 μA cm^{-2} mM^{-1} [21], AuNW at 15.6 μA cm^{-2} mM^{-1} [28], and PPyNT at 7.4 μA cm^{-2} mM^{-1} [30]. Even with the use of applied potentials of 500 and 300 mV with the PPyNWA–PtNPs–GOx biosensor, the achieved sensitivities of 29 and 24 μA cm^{-2} mM^{-1}, respectively, were still much better. The achieved detection limit (3σ) of 27.7 μM with the PPyNWA–PtNPs–GOx biosensor is also better than those reported with other nanomaterials such as AuNW at 46 μM [28], and PPyNT at 108 μM [30], but not as good as that (5.6 μM) achieved by potentiometric detection in this study. This superior detection limit obtained with the potentiometric detection is due to the ability of the hydrogen peroxide produced from the enzyme catalysed oxidation of glucose to cause significant potential change and, thus, result in a higher sensitivity. This has been shown to result in the attainment of super-Nernstian response for glucose [26] and, thus, can lead to improved detection limit. Further improvement in the sensitivity and achievable detection limit by both amperometric and potentiometric detection of glucose with the PPyNWA–PtNPs–GOx biosensor can be realized

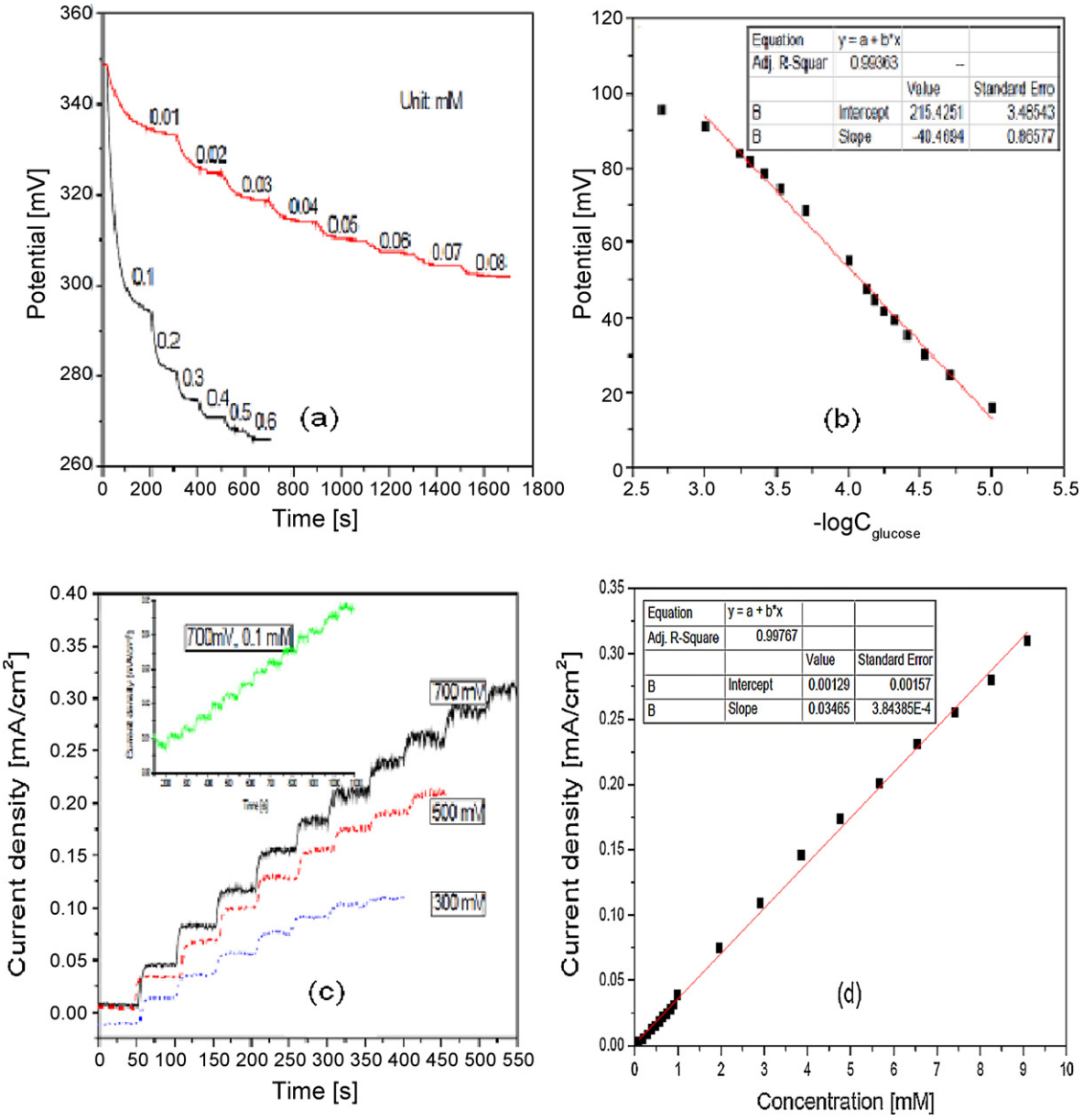

Fig. 4. Potentiometric and amperometric detection of glucose with the PPyNWA–PtNPs–GOx biosensor. (a) Chronopotentiograms for increasing glucose concentrations, (b) Nernstian plot, (c) chronoamperograms for increasing glucose concentrations at different applied potentials, and (d) typical calibration curve. Measurement in 0.05 M phosphate buffer (pH 7.0). For (c), each addition of glucose for inset is 0.1 mM, and for others (black, blue and red traces) is 1 mM.

by immobilization of the enzyme by direct entrapment into the PPy–NWA or on top of the PtNPs. Both of these approaches are currently being investigated in our laboratories to enable reliable application of the PPyNWA–PtNPs–GOx biosensor to real samples.

4. Conclusions

Fabrication of a well aligned PPyNWA with a diameter of about 20 nm within AAO template has been successfully demonstrated. The electrochemical properties of the PPyNWA were significantly enhanced by decoration with PtNPs via cyclic deposition. Adsorption of GOx over the PPyNWA–PtNPs enabled both amperometric and potentiometric detection of glucose. The potentiometric detection achieved much lower detection limit (5.6 μM) than with amperometric detection (27.7 μM). However, the response time for the latter (~7 s) was much faster than for the former (>100 s). Based on detection limit and linear concentration range, the use of the PPyNWA–PtNPs–GOx biosensor in the potentiometric mode is superior than the amperometric mode, but can be used complementarily to detect low (10 μM to 1 mM by potentiometric mode) and high (0.1 mM to 9 mM by amperometric mode) glucose concentrations. The possibility of achieving further improvement in sensitivity and detection limit by both detection modes via direct entrapment of GOx within PPyNWA or on top of PPyNWA–PtNPs is currently being investigated.

Acknowledgements

G.Q. Xu is grateful to the School of Applied Sciences and Engineering for supporting his research visit and thanks Mr. Kamran Khajehpour for providing assistance with scanning electron microscopy measurement. This work was also supported by Nature Science Foundation of China (51102071, 51072044) and China Postdoctoral Science Foundation (20100480678).

References

[1] T.W. Tsai, G. Heckert, L.F. Neves, Y.Q. Tan, D.Y. Kao, R.G. Harrison, D.E. Resasco, D.W. Schmidtke, Anal. Chem. 81 (2009) 7917.
[2] X.Y. Pang, D.M. He, S.L. Luo, Q.Y. Cai, Sens. Actuators B 137 (2009) 134.
[3] Z.J. Zhang, Y.B. Xie, Z. Liu, F. Rong, Y. Wang, D.G. Fu, J. Electroanal. Chem. 650 (2011) 241.
[4] A.W. Shi, F.L. Qu, M.K. Yang, G.L. Shen, R.Q. Yu, Sens. Actuators B 129 (2008) 779.
[5] J. Li, X.Q. Lin, Sens. Actuators B 126 (2007) 527.
[6] C.Y. Wang, S.H. Chen, Y. Xiang, W. Li, X. Zhong, X. Che, J. Li, J. Mol. Catal. B 69 (2011) 1.
[7] N. Chauhan, C.S. Pundir, Anal. Biochem. 413 (2011) 97.
[8] H. Park, T.J. Park, Y.S. Huh, B.G. Choi, S. Ko, S.Y. Lee, W.H. Hong, J. Colloid Interface Sci. 350 (2010) 453.
[9] S.Q. Liu, A.C. Chen, Langmuir 21 (2005) 8409.
[10] S.X. Huang, Y. Chen, Nano Lett. 8 (2008) 2829.
[11] M. Stoces, K. Kalcher, I. Svancara, K. Vytras, Int. J. Electrochem. Sci. 6 (2011) 1917.
[12] A.T. Lawal, S.B. Adeloju, J. Mol. Catal. B 63 (2010) 45.
[13] M. Sohail, S.B. Adeloju, Electroanalysis 21 (2009) 1411.
[14] C. Debiemme-Chouvy, Biosens. Bioelectron. 25 (2010) 2454.
[15] M. Zhao, X.M. Wu, C.X. Cai, J. Phys. Chem. C 113 (2009) 4987.
[16] K. Ghanbari, S.Z. Bathaie, M.F. Mousavi, Biosens. Bioelectron. 23 (2008) 1825.
[17] L. Liu, C.J. Zhao, Y.M. Zhao, et al., Eur. Polym. J. 41 (2005) 2117.
[18] D.J. Shirale, M.A. Bangar, W. Chen, N.V. Myung, A.J. Mulchandani, J. Phys. Chem. C 114 (2010) 13375.
[19] G.H. Zhao, Y.Z. Lei, Y.G. Zhang, H.X. Li, M.C. Liu, J. Phys. Chem. C 112 (2008) 14786.
[20] M. Hosseini, M.M. Momeni, J. Solid State Electrochem. 14 (2010) 1109.
[21] J. Li, X.Q. Lin, Biosens. Bioelectron. 22 (2007) 2898.
[22] X.Y. Jiang, Y.H. Wu, X.Y. Mao, X. Cui, L. Zhu, Sens. Actuators B 153 (2011) 158.
[23] J.J. Lingane, J. Electroanal. Chem. 7 (1964) 94.
[24] F.A. Adekola, C. Colin, D. Bauer, Electrochim. Acta 37 (1992) 507.
[25] K.B. Male, S. Hrapovic, J.H.T. Luong, Analyst 132 (2007) 1254.
[26] S.B. Adeloju, A.N. Moline, Biosens. Bioelectron. 16 (2001) 133.
[27] A. Halder, S. Sharma, M.S. Hegde, N. Ravishankar, J. Phys. Chem. 113 (2009) 1466.
[28] X.Y. Zhang, D. Li, L. Bourgeois, H. Wang, P.A. Webley, Chem. Phys. Chem. 10 (2009) 436.
[29] R.B. Rakhi, K. Sethupathi, S. Ramaprabhu, J. Phys. Chem. B 113 (2009) 3190.
[30] E.M.I.M. Ekanayake, D.M.G. Preethichandra, K. Kaneto, Biosens. Bioelectron. 23 (2007) 107.